Image Denoising with Grouplet Transform

Jingwen Yan, Zhixi Wang, Longquan Dai, Daxiang Huang
Department of Electronic Engineering
Shantou University, Shantou
Guangdong, China
07zxwang1@stu.edu.cn

Abstract—**Grouplet transform(GT) can take advantage of the image's geometry structure since the bases of Grouplet can adapt the different geometry structure in different scales. The association fields that calculate by The Block Matching algorithm which cannot adaptive to different textures cannot follow the turbulent texture contained in an image. Grouplet transform based on Streamline (GTS) introduced streamline to improve the performance of represent of turbulent texture. The starting pixel selected for association fields pruning was arbitrary, and one flow will prune to several flows that would destroy the original texture decreased the performance of Grouplet Transform. This paper proposed an advanced grouplet transform (AGT) that make use of the advantage of Greedy algorithm and Dynamic Programming algorithm in association fields pruning to ensure association fields well suited of the image's texture structure. Experimental results show that the performance of image denoising by AGT-threshold outperforms GT-threshold denoising method and GTS-threshold denoising method.**

Keywords- Grouplet transform; Stream; Greedy algorithm; Dynamic programming algorithm.

I. INTRODUCTION

Nature images are decomposed of many areas that contained geometric structures. Figure 1 shows some examples of geometric structures contained in nature images. These geometric structures provide fundamental features for many problems in computer vision and image processing [1], and understanding how to represent complex geometric structures is the key to improve state of the image processing.

Wavelet bases that can adapt the resolution of image approximations depending upon the local image regularity are particularly to represent images [2]. Since their square support is not adapted to directional geometric structures, wavelet bases are suboptimal to represent images that contain complex geometrical structures. GT was proposed by Mallat to represent complex geometric structures. In the spirit of the "Gestalt" psychophysic school[3]-[6], the geometry is constructed with grouping processes which define multiscale association fields[7]. GT was a new transform that it's bases can adapt to geometric textures in directional scales, and it can make the most effective use of geometric structures. GTS introduced stream to calculate association fields and make a better performance than GT in represent images contain complex geometric structure.

This paper introduces Greedy algorithm and Dynamic Programming algorithm in association fields pruning to ensure association fields well suited for images contain complex textures. Section II describes the coefficient layer computation of GT. Section III describes the association field layer computation of GT and introduces Greedy algorithm and Dynamic Programming algorithm in association field pruning. Applications are described in section IV to remove noise from images and restore more details than GT and GTS.

II. GROUPLET COEFFICIENTS LAYER COMPUTATION

A. Forward decomposition

Grouplet decompose an image F into multiscale difference coefficients and coarse scale average coefficients. We can get these coefficients from successive grouping and computation according to multiscale association fields. Suppose that F includes N samples. Define an ordering fuction $\alpha(n)$ that is compatible with the grouplet partial ordering. Invertible mapping $\alpha(n)$ associates to any integar $1 \le n \le N$, a point $m = \alpha(n)$ such that if $m = \alpha(n)$ is before $p = \alpha(u)$ with respect to the grouplet partial ordering, then $n < u$.

Create a new array s[n] to store the support size of the averaging coefficients of image F. Initialize $a = F$; $\forall m \in F, s[m] = 1$. F is decomposed into multiscale difference layers $\tilde{F}_j$ and coarse scale average layer F_J. Each scale normalized difference coefficients and average coefficients is

$$d_j[\tilde{m}] = (a[\tilde{m}] - a[m]) \frac{\sqrt{s[m]s[\tilde{m}]}}{\sqrt{\hat{s}}} \tag{1}$$

$$\hat{a} = \frac{s[m]a[m] + s[\tilde{m}]a[\tilde{m}]}{\hat{s}} \tag{2}$$

and the averaging size is update by adding the averaging size of the two averaged points: $\hat{s} = s[m] + s[\tilde{m}]$. At the coarsest scale 2^J, the average coefficients are normalized: $a_J[m] = a[m]\sqrt{s[m]}$.

B. Backward decomposition

Image can be reconstructed from it's grouplet coefficients and association field.

978-1-4244-5848-6/10/$26.00 ©2010 IEEE

The average coefficient normalization is then inverted: $\forall m \in A_J$, $a[m] = \frac{a_J[m]}{\sqrt{s[m]}}$, each grouping operator is then inverted in the reverse order it was calculated. For j decreasing from J to 1 and for n going from N to 1:

$$\tilde{s} = s[m] - s[\tilde{m}] \quad (3)$$

$$\tilde{a}_- = a[m] + d_j[\tilde{m}] \frac{\sqrt{\tilde{s}}}{\sqrt{s[\tilde{m}]s[m]}} \quad (4)$$

$$\tilde{a}_+ = a[m] - d_j[\tilde{m}] \frac{\sqrt{s[\tilde{m}]}}{\sqrt{\tilde{s}s[m]}} \quad (5)$$

$$\tilde{a} = \frac{\tilde{a}_- + a[\tilde{m}]}{2} \quad (6)$$

A causal reconstruction recovers the average value at $\tilde{m}$ from a coefficient located before m in equation (4). An anti-causal reconstruction recovers the average value at m from a coefficient located after m in equation (5). Equal averaging weights on causal and anticausal reconstructions implement the pseudo-inverse in equation (6). The averaging size is then updated $s[m] = \tilde{s}$. At the end of loop over all j and n, this left inverse reconstructs image F.

III. GROUPLET ASSOCIATION FIELD LAYER COMPUTATION

For a giving image $F \in R^2$ that has $N = n \times n$ pixels, we need to estimate the local texture orientation Γ . Geometric structures in a locally parallel texture do not have a specific direction, the local orientation we computed has two directions: $\Gamma_{(x)}$ and $-\Gamma_{(x)}$, both of them are equally suitable to represent the texture.

A. Local Orientation Field Computation

Image F's local direction of the edges are captured by the vector v(x) that is orthogonal to the gradient $\nabla_x F$.

$$v = \nabla_x A^{\perp} = (\frac{\partial F}{\partial x} i + \frac{\partial F}{\partial y} j)^{\perp} = -\frac{\partial F}{\partial y} i + \frac{\partial F}{\partial x} j, \forall x \in F \quad (7)$$

Vector v(x) is suitable to represent the direction of step edges in images, but it cannot be used directly to represent the orientation of locally parallel textures, since it vanishes at the top of ridges or at the bottom of valleys. This problem can be alleviated by pooling locally the orientation information, The local non-linear pooling corresponds to a local covariance analysis, summing the outer products of gradient vectors in a local region to generate a tensor field[9]-[11]. Specially, the structure tensor T_{f_0} is defined as a local averaging of the rank-1 tensor field vv^T :

$$T_{F(x)} = (G_\delta * (vv^T))(x) = G_\delta * \begin{pmatrix} v_1^2 & v_1 v_2 \\ v_1 v_2 & v_2^2 \end{pmatrix}(x) \quad (8)$$

where $G_\delta(x) = \frac{1}{\varepsilon\sqrt{2\pi}} \exp(-\frac{x^2}{2\delta^2})$, and the convolution is applied on each component of the tensor. Figure 3 shows some tensor field of images.

Each symmetric tensor $T_{F(x)}$ is decomposed as a sum of two rank-1 tensors:

$$T_{F(x)} = \lambda(x)(\Gamma(x)\Gamma(x)^T) + \lambda^{\perp}(x)(\Gamma^{\perp}(x)\Gamma^{\perp}(x)^T) \quad (9)$$

Where the eigenvalues of $\lambda(x) \geq \lambda^{\perp}(x) \geq 0$ and $\left(\Gamma(x), \Gamma^{\perp}(x)\right)$ are the corresponding orthogonal eigenvectors. The dominant eigenvector $\Gamma(x)$ indicates the local direction of the texture.

B. Local Directional Vector Field Computation

The orientation field $\Gamma(x)$ is used to describe the geometry texture of an image. It is necessary to find a smooth directional vector field $\tilde{\Gamma}(x) = \varepsilon(x)\Gamma(x)$, where $\varepsilon(x) \in \{-1, +1\}$. In general it is not possible to find a globally smooth vector field $\tilde{\Gamma}$ in the sense of topological incompatibilities. However we can find a suitable vector field outside the set of structural singularities [2] which are given by the set of separatrices $S(\Gamma)$.

Each separatrix link together two umbilic points of Γ is a stream line γ that parallel to Γ :

$$\forall t. \ \left|\left\langle \gamma'(t), \Gamma(\gamma(t)) \right\rangle\right| = \left\|\gamma'(t)\right\| \quad (10)$$

The sign field ε is found by optimizing the smoothness of $\tilde{\Gamma} = \varepsilon\Gamma$ outside $S(\Gamma)$. In the discrete setting, one solves the following minimization

$$\min_{\varepsilon} \sum_x \left\| \varepsilon(x)\Gamma(x) - \frac{1}{|V_x|} \sum_{y \in V_x} \varepsilon(y)\Gamma(y) \right\|^2 \quad (11)$$

where $y \in V(x)$ is a direct neighbor of a pixel x.

$$\begin{cases} \forall x, \quad \varepsilon(x) = \dfrac{1}{|V_x|} \displaystyle\sum_{y \in V_x} \varepsilon(y) \left\langle \Gamma(x), \Gamma(y) \right\rangle \\ s.t. \ \ \forall x, \quad \tilde{\Gamma}(x) = sign(\varepsilon(x))\Gamma(x) \end{cases} \quad (12)$$

In order for the equation (12) to be uniquely solvable, one needs to set additional constraints $\varepsilon(x) \in \{-1, +1\}$ to $\varepsilon \in R$, where each pixel $z_i \in C_i$ belongs to a cell of the separatrices segmentation.

Equation (12) requires to solve a sparse linear system and the un-signed orientation field is then turned into a signed vector field that defines the local direction of the geometric:

$$\forall x, \quad \tilde{\Gamma}(x) = sign(\varepsilon(x))\Gamma(x) \quad (13)$$

C. Association Field Computation and Pruning

After discretizing and pruning the local field Γ, we can get a set of association fields $\{A_l\}_{l=0}^{L-1}$. At the scale 2^l, each association field A_l groups together two points $x \to y = A_l(x)$ that are separated by a distance of approximately $\|x-y\| \approx 2^l$. Suppose that $\psi_{(x)} = \{y | A_l(x) = y\}$ is the set of points y that are grouped by points x at scale 2^l; $\zeta_{(x)} = \{z_i | A_l(z_i) = x,\ i = 1, \cdots n\}$ is the set of points z_i that grouping points x at scale 2^l; select a point z_i that has the most times be grouped in the set, signed it $\max \zeta_{(x)}$.

It is important to note that our construction of the association field differs from the ones of [12] and [13], and the construction of the association field of [12] is based on a fixed directional ordering of the grid points, that forbids an arbitrary association field, that is not well suited to process turbulent textures. Literature [13] introduced streamline to construct association field, it can adapt estimates the geometric flow of the texture and represent efficiently the texture of image. However in the process of association field pruning, the selection of original starting point is arbitary, it may break off one streamline to several streamlines. In this paper, we take the advantage of Greedy algorithm and Dynamic Programming algorithm[14] in association fields pruning to ensure the starting point is the original starting point and prevent prune one streamline to several streamlines, it is better suited the texture than the ones in [12] and [13].

The directional vector field $\tilde{\Gamma}$ computed in section III-B serves as a seed for the following linear differential flow:

$$\forall x, \forall t > 0, \frac{d\varphi_x}{dt} = \tilde{\Gamma}_{(\varphi_x(t))}, \quad \varphi_x(0) = x \tag{14}$$

Interpolate the field to solve numerically this ordinary differential equation. Each integral curve $\{\varphi_x(t)\}_{(t>0)}$ follows the vector field $\tilde{\Gamma}$ and is also a flow line of Γ. A raw discrete association field A_l^0 at various scales l is gotten by sampling this integral curve at dyadic locations:

$$\forall x, \quad A_l^0(x) = [\varphi_x(2^l)]_{n \times n} \in \{0, \ldots, n-1\}^2 \tag{15}$$

where $[\cdot]_{n \times n}$ is the rounding operator that projects the points on the sampling grid $\{0, \ldots, n-1\}^2$.

Starting from this row association field, one computes a 1D ordering of the grid points $V_l : \{0, \ldots, n-1\}^2 \to \{0, \ldots, N-1\}$, where $N = n^2$, that orders the points for the computation of the GT. For each l, the ordering V_l tries as much as possible to be coherent with the associations created by A_l^0, and looks for a pruned association field A_l closed to the raw field together with an ordering V_l that satisfies $\forall x, \quad A_l(x) \neq x \ \Rightarrow \ V_l(A_l(x)) < V_l(x)$. Excepted at a few singular points where $A_l(x) = x$, the association field A_l links points with increasing values of the ordering function V_l. The hybrid algorithm with the advantage of Greedy algorithm and Dynamic Programming algorithm to prune a raw association field is

Input: raw association field A_l^0.

Output: pruned association field A_l and coherent ordering V_l.

1) Initialization:
$A_l = A_l^0; j = 100000; k = 0; \forall x, V_l(x) = -1$. For each x, build the father list $\psi_{(x)}$ and son list $\zeta_{(x)}$.

2) Select a point: choose some x satisfyied $V_l(x) = -1$;

3) Initialize $W = V_l$, if $W(\psi_{(x)}) < 0$, do
$A_l(x) \leftarrow x, w(x) \leftarrow j$.

4) Search original starting point:
initialize the pool: $P = \{x\}$.
if $P \neq \varnothing, \xi(x) < 0$, do
extract $x \in P$, remove $P \leftarrow P / x$;
set: $P \leftarrow \max \zeta_{(x)}$; $j \leftarrow j - 1$, $W(z) \leftarrow j$.

5) stop : if $W_l(z) < 0 = \varnothing$, return x; goto 6).

6) Set up the ordering:
initialize the pool: $\tilde{P} = \{x\}, V_l(x) \leftarrow k$
if $V_l(\psi(x)) < 0$, do
$k \leftarrow k + 1, V_l(\psi(x)) \leftarrow k$; remove x: $P \leftarrow P / x$;
set: $P \leftarrow y$.

7) Stop: if $0 \le V_l(\psi(x)) < V_l(x)$ goto 2).

8) Prune the flow: $for\ all\ x:\ V_l(\psi(x)) > V_l(x)$,
do $A_l(x) \leftarrow x$.

The value of j at step 1) depends upon the total number of pixels in the image that we used in our experiment. The size of image is 128×128, we set j to 100000 that bigger than 128×128 to ensure we can find the original starting point, we build the father list and son list of x to search the original starting point of the flow that contain pixel x. The hybrid algorithm with the advantage of Greedy algorithm and Dynamic Programming algorithm was used to search the original starting point of one flow at step 2) to 5), and Step 4) ensures each flow we find is the longest one of all. Step 5) ensure we find the original starting point, then go to step 6) to prune this flow. The follow is pruning over if conditions satisfy step 7), then go to step 2) to prune other flows. At the end of this loop, all the flows have been pruned

and formed the pruned association field A_l and coherent ordering V_l .

IV. EXPERIMENTAL RESULTS AND CONCLUSIONS

We experiment with the image Fig. 1. (a) shows that contains rich textures which size was 128×128 . The image was decomposed by GT, GTS and AGT and AGT, searching for one of these association fields that are most suitable with the original texture, then add additive Gauss noise to the original image and denoised with hard-threshold method, compared the performance of GT, GTS and AGT in denoising application[15]. The threshold $T(\alpha)=r\times\sigma_n^2/\sigma_x$, where σ_n is noise standard deviation, σ_x is signal standard deviation, r is a controllable parameter. The denoising effect is perfect when we set the value of r to about 3.3, which has been validated by many times experiments.

Figure 4 shows the associations fields of image that transform by GT, GTS and AGT. The follows are conclusions from the experimental results:

1) As shown by Fig. 4. (d), the association field transformed by GT is well suited the horizontal direction textures of image, cannot well suited the vertical direction textures, especially for the regions that contain turbulent textures.

2) The association field transformed by GTS well suited not only the horizontal direction textures but also the vertical direction textures in the regions that contain turbulent textures, as shown by Fig. 4. (e). However one flow disjoins into too many flows and destroyed the texture structure of image.

3) The association field transformed by AGT has a better perform on represent the textures of image than GT and GTS, especially for the for the regions that contain abundance textures. The representation of texture is more flexible than GTS since we avoid disjoin one flow to several flows, as shown by Fig. 4. (f).

Figure 5 shows the image that transformed by GT, GTS and AGT, then denoised by hard threshold. The PSNR of noised image is 18.5 dB, as shown by Fig. 5. (b). The follows are conclusions from the experimental results:

1) The PSNR of image that transformed by GT and denoised by hard threshold is 23.4 dB, and has about 5 dB advance compare to noised image. The denoising effect is obviously and attests the potential of GT in image deonising application. However the denoised image loses many textures of original image, since the computation of association field can't adapt the structure of image, as shown in Fig. 5. (c).

2) The PSNR of image that transformed by GTS and denoised by hard threshold is 24.7 dB, and has about 1.3 dB advance compare to GT-threshold denoising, and the lose of textures is less than GT-threshold denoising, as shown in Fig. 5. (d). This owed to the introduce of flow to the computation to association field.

3) The PSNR of image that transformed by AGT and denoised by hard threshold is 26.2 dB, and has about 1.5 dB advance compare to GTS-threshold denoising, and the lose of textures is the least one of all denoising methods im this paper, as shown in Fig. 5. (e). Form the comparison of the region in (c), (d) and (e) that correspond to the region in the red rectangle in Fig. 5. (a), we can see that the AGT-threshold denoising method can preserve more details than other methods used in this paper.

In this paper, we improved the computation of association field by introducing Greedy algorithm and Dynamic Programming algorithm in the pruning of association fields to avoid disjoin one flow to several flows. The results of numerical experiments show that the representation of image improved by this paper better suited the textures than GT and GTS. We proposed a novel denoising method based on AGT for grometrical image, and compared with GT-threshold and GTS-threshold, the results show that the PSNR of image denoised by AGT-threshold is obviously improved in comparison with other methods, and preserve more textures than other methods.

The AGT, a fast transform and provide sparse representation of directional textures, will be applied widely in the future, such as image inpainting, SAR image denoising, medical imaging, image enhancement, image compression based on texture, image analysis and so on. How to use it to image processing application widely will be the emphasis of our research in the future.

ACKNOWLEDGMENT

The paper is supported by Navigation Science Foundation of China (No.05F07001) and Nation Natural Science Foundation of China (No. 40971206). Prof. Yan, as advisor of mine, is corresponding author. I am sincerely got the grateful for his help. And I would like to thank very much Longquan Dai for his cooperation and helpful suggestion. At the end, I thank the other group team members for their support and help.

[1] J. R. Bergen and M. S. Landy, "Computational modeling of visualtexture segregation," in Comp. Models of Visual Proc., M. S. Landy and J. A. Movshon, Eds. Cambridge, MA: MIT Press, 1991, pp. 253–271.

[2] E. Le Pennec and S. Mallat, "Bandelet Image Approximation and Compression," SIAM Multiscale Modeling and Simulation, 4(3) :992-1039, 2005.

[3] P. C. Bressloff and J. D. Cowan. The functional geometry of local and horizontal connections in a model of V1. J Physiol Paris, 97(2-3): 221-236, Mar-May 2003.

[4] Kanizsa G. Organization in Vision: Essays on Visual Perception. Praeger, 1979.

[5] D. J. Heeger, E. P. Simoncelli, and J. A. Movshon. Computational models of cortical visual processing. Proc National Academy of Science, 93: 623-627, 1996.

[6] R. F. Hess, A. Hayes, and D. J. Field. Contour integration and cortical processing. J Physiol Paris, 97(2-3): 105-119, Mar-May 2003.

[7] D. J. Field, A. Hayes, and R. F. Hess. Contour integration by the human visual system: evidence for a local "association field". Vision Research, 33(2): 173-193, 1993.

[8] L. Luo, F. Wu, S. Li, and Z. Zhuang, “Advanced lifiting-based motion_threading technique for the 3-d wavelet video coding,” Processing. Academic Press, San Diego, 1999.

[10] U. Kothe, “Edge and junction detection with an improved structure tensor,” in Proc. DAGM03, 2003, pp. 25–32.

[11] A. Rao and R. Jain, “Computerized flow field analysis: Oriented texture fields,” IEEE Transactions on Pattern Analysis and Machine Intelligence,vol. 14, no. 7, pp. 693–709, 1992.

[12] S. Mallat, “Geometrical grouplets,” to Appear in Applied and Computational Harmonic Analysis, 2008.

[13] G.. Peyre, “Texture Synthesis with Grouplets,” IEEE Transactions on Pattern Analysis and Machine Intelligence, volume PP, Forthcoming, page(s). 1–1, 2009.

[14] Thomas H. Cormen, Charles E. Leiserson, Ronald L. Rivest and Clifford Stein, “Introduction to Algorithms,” Second Edition, MA: MIT Press, 2001, pp. 370–399.

[15] S. G. Chang, B. Yu, M. Vetterli. Image denoising via lossy compression and wavelet thresholding [J]. IEEE Trans. Image Processing, 2000, 9(1): 1532–1546.

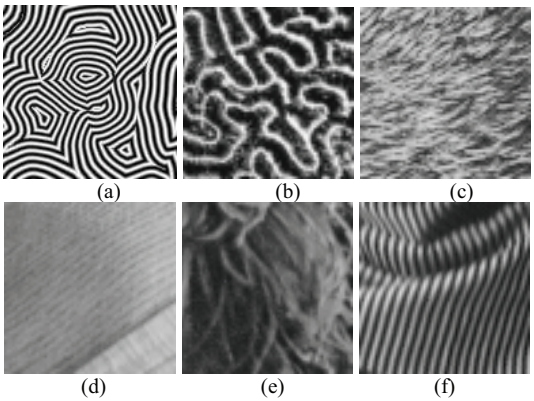

Figure 1. Geometric structure of nature images.

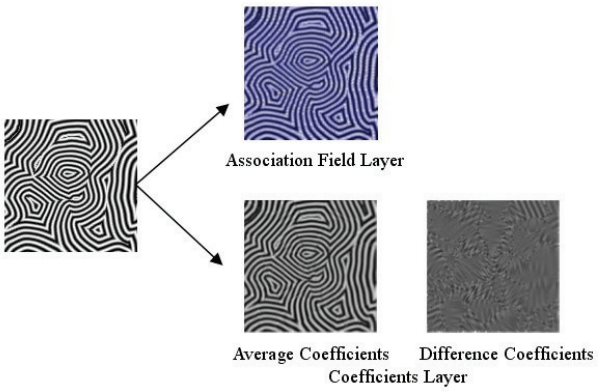

Fig. 2. Grouplet decomposition of composes of association field layer computation and coefficient layer computation.

[9] M. Kass and A. Witkin, “Analyzing oriented patterns,” Comput. Vision Graph. Image Process., vol. 37, no. 3, pp. 362–385, 1987.

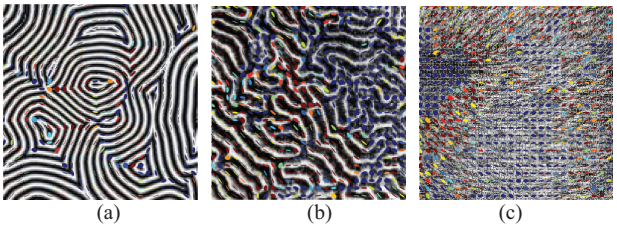

Fig. 3. Structure tensor field $T_{f0.}$

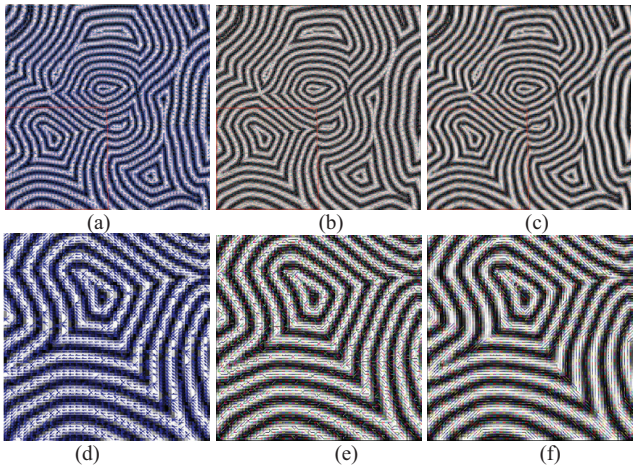

Fig. 4. Association fields of image. (a) Association field of image transform by GT; (b) Association field of image transform by GTS; (c) Association field of image transform by AGT; (d), (e),(f) is the area that shown in red rectangle of (a), (b), (c) separately.

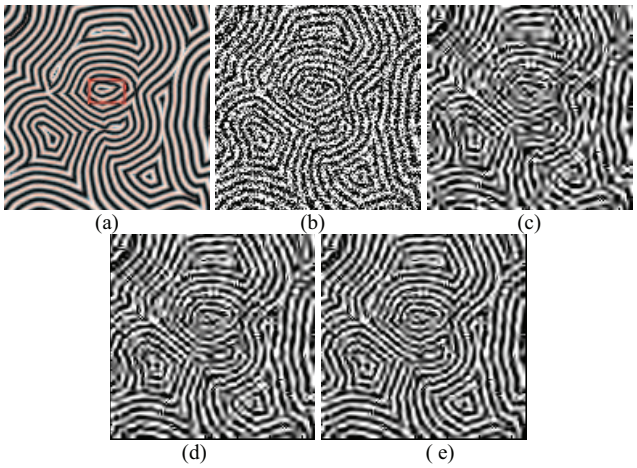

Fig. 5. Denoise results (a) Original image; (b) Noised Image (PSNR=18.5dB); (c) Denoised Image by GT-threshold (PSNR=23.4dB); (d) Denoised Image by GTS-threshold (PSNR=24.7dB); (e) Denoised Image by AGT-threshold (PSNR=26.2dB).